

# Experimental Investigation of Coupled Ferrite-Dielectric Image Guide Structure in Ka-band

Iliyana Arestova, Rositsa Tomova

**Abstract:** Coupled ferrite and dielectric image guides with nonreciprocal behavior in Ka-band (26–38 GHz) have been investigated experimentally with the help of electric probes. The ferrite element has been magnetized inhomogeneously by a disk-shaped permanent magnet. The distributions of all three electric field components in forward and backward direction of propagation have been measured along the coupling length. Examination of measured distributions permit to clarify the operating mechanism of the nonreciprocal ferrite-dielectric structure. This structure can be used for design of nonreciprocal devices, namely isolators for this part of millimeter wave range.

**Index Terms:** Coupled Image Guide Structures, Image Guide, Ferrite Materials, Nonreciprocal Devices, Millimeter Waves.

## I. INTRODUCTION

Interest in millimeter-wave range is kept permanently high over the past decades. Full use of the millimeter range implies its provision with all necessary active and passive, reciprocal and nonreciprocal devices. Nonreciprocal devices, in particular, have been traditionally invented on the basis of magnetized ferrite elements. The ferrite materials unfortunately decrease their gyrotropy as the frequency is increased. That is the reason the conventional ferrite devices developed for lower frequencies (centimeter-wave range) cannot be used with the same success in millimeter-wave range. Alternative approaches are sought to invent nonreciprocal devices for millimeter-wave range, which require only weak gyrotropy [1].

One of these alternative approaches is the achievement of nonreciprocal behavior of coupled ferrite-dielectric image guide (CFDIG) structures [2]–[4]. Three mutually perpendicular directions of homogeneous magnetization of the ferrite image guide (IG), which couples two lateral dielectric IGs, have been investigated in [2]. Nonreciprocal effects have been registered at all directions of magnetization, but relatively high permanent magnetic fields have been needed, that leads to large magnetic systems.

Very good nonreciprocal parameters have been reported in [3], [4] for a CFDIG structure with inhomogeneously magnetized ferrite element (bar). It has been magnetized by using a disk-shaped permanent magnet, whose diameter is comparable with the length of the ferrite bar. The clarification of the operating mechanism of such type CFDIG devices represents a complex problem due to the inhomogeneity of the ferrite magnetization and the effects taking place at the ends of coupling length. Here we have completed experimental investigation of the electric field components along the coupling length by using electric probes. The distributions of all three electric field components have been measured and conclusions about the operating mechanism have been made.

## II. CONFIGURATION OF THE CFDIG STRUCTURE

The configuration of the CFDIG structure under investigation is shown in Fig. 1. The primary IG 1 has transverse dimensions  $a \times b = 2.00 \text{ mm} \times 0.97 \text{ mm}$  (Fig. 1b). It is made by alumina with a relative permittivity  $\epsilon_r = 9.6$  and a dielectric loss tangent  $\text{tg}\delta_\epsilon = 10^{-4}$ . The secondary IG with transverse dimensions  $a_f \times b_f = 2.20 \text{ mm} \times 1.10 \text{ mm}$  is made by nickel ferrite (1C44, Russia). The ferrite has a relative permittivity  $\epsilon_r = 11.1$ , a dielectric loss tangent  $\text{tg}\delta_\epsilon = 10^{-2}$  and a saturation magnetization  $4\pi M_s = 4.63 \text{ kG}$ . The primary and secondary IGs are stuck on the metal (ground) plate 3. They are coupled each to other on a coupling length  $l$  equal to 17.6 mm (Fig. 1a). The metal plate 3 represents parallelepiped with dimensions  $49 \text{ mm} \times 9 \text{ mm} \times 80 \text{ mm}$ , which contains on its bottom center a cylindrical channel with diameter 32 mm and depth 8 mm. The axis of the cylindrical channel is along  $Oy$  axis (Fig. 1b). This channel permits positioning of the permanent magnet under the ground plane.

There are two transitions 4 on both ends of the primary IG which perform a conversion of the dominant mode  $H_{10}$  on the standard metal rectangular waveguide (SMRW) to the mode  $E_{y11}$  on the rectangular IG (according to Marcattilli's classification [5]). The transitions are performed by a symmetrical tapering of the dielectric bar in  $xz$  plane and thereafter putting the tapers into SMRW sections of the same length. The whole length of the test structure was 80 mm including both 15 mm transitions. The transverse surfaces of the transitions were coated with absorbing plates 5 in order to minimize undesirable reflections.

Manuscript published on 30 October 2018.

\* Correspondence Author (s)

Iliyana Arestova, Department of Radiophysics and Electronics, Faculty of Physics, St. Kliment Ohridski University of Sofia, 5 James Bourchier Blvd., 1164 Sofia, Bulgaria, E-mail: [ilar@phys.uni-sofia.bg](mailto:ilar@phys.uni-sofia.bg)

Rositsa Tomova, Atanas Damyanov Vocational High School, 2 Osvobogdenie Street, 6190 Nikolaevo, Bulgaria. E-mail: [tomova\\_rossi@mail.bg](mailto:tomova_rossi@mail.bg)

© The Authors. Published by Blue Eyes Intelligence Engineering and Sciences Publication (BEIESP). This is an [open access](https://creativecommons.org/licenses/by-nc-nd/4.0/) article under the CC-BY-NC-ND license <http://creativecommons.org/licenses/by-nc-nd/4.0/>.

## Experimental Investigation of Coupled Ferrite-Dielectric Image Guide Structure in Ka-band

The main difference of the configuration shown in Fig. 1a in comparison with those in [3], [4] is its uniformity along the coupling length. Both ends of the ferrite element in [3], [4] have been tapered in  $xz$  plane in order to diminish

reflections and to improve matching. Here we have chosen the uniform

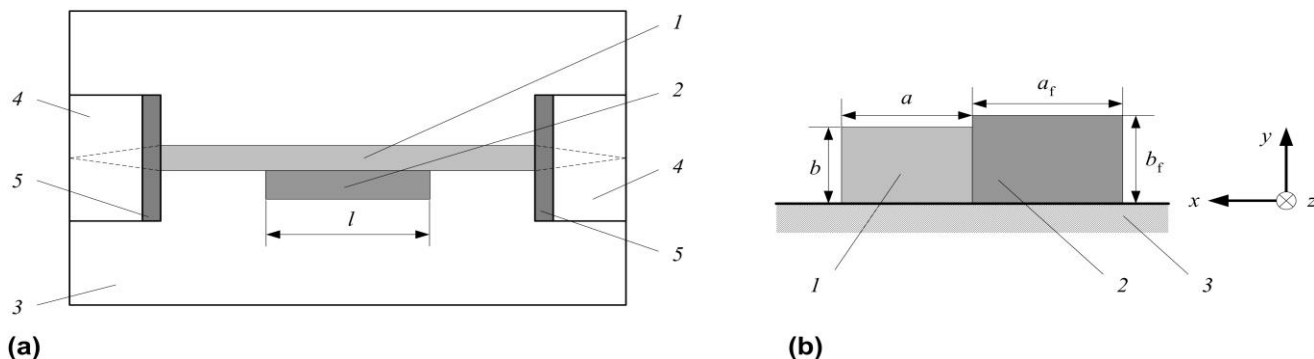


**Fig. 1. Configuration of the CFDIG structure.**

(a) top view; (b) cross sectional view.

1 – primary IG; 2 – secondary IG; 3 – metal plate; 4 – SMRW-IG transition; 5 – absorbing plates.

configuration of the coupled region to make the process of coupling simpler bearing in mind that this could worsen the matching.

### III. EXPERIMENTAL SETUP AND ELECTRIC PROBES

The experimental setup used is shown in Fig. 2a. The scalar network analyzer 1 works in Ka-band (26–38 GHz) and includes SMRW components with a cross section of  $7.2 \text{ mm} \times 3.4 \text{ mm}$ . The generator 2 can operate both in a swept and in a fixed frequency mode. The directional couplers 4 combined with the build-in detectors 5 permit a separation of the incident and the transmitted wave to and out of the structure under investigation 6. The configuration of the electric probes 7 used for the electric field sampling is shown in Fig. 2b. Two different probes have been used – the probe shown in the left has been used for the  $E_y$  component, and the one shown in the right – for both  $E_x$  and  $E_z$  components at the proper orientation. The electric probe for the  $E_y$  component contains a straight vertical section of the

inner conductor, while the electric probe for  $E_x$  and  $E_z$  – a  $90^\circ$  bend section. Both electric probes represent a section of a semi-rigid coaxial cable ( $50 \Omega$ , outer diameter 2.20 mm), which has its outer conductor removed at both ends on the length of about a quarter of a wavelength. One of the ends of the coaxial cable has been inserted into a hole in the middle of the broad wall of a SMRW section. One of the ports of the SMRW section has been shorted at about a quarter of a wavelength, and the second port has been connected with a waveguide detector 8. The output of the detector has been connected to the DC microvoltmeter 9, which has been used as an indicator. The electric probe has been mounted on a three axes mechanism described in details in [6]. It permits probe positioning with an accuracy of 0.05 mm along the longitudinal axis  $Oz$  and 0.01 mm along the transverse axes  $Ox$  and  $Oy$ . The finite dimensions of the electric probes – a diameter of 0.51 mm and a length of about 2 mm, determine the accuracy of the electric field sampling. The diameter of the probe is much lesser than the guide wavelength and may not be taken into account.

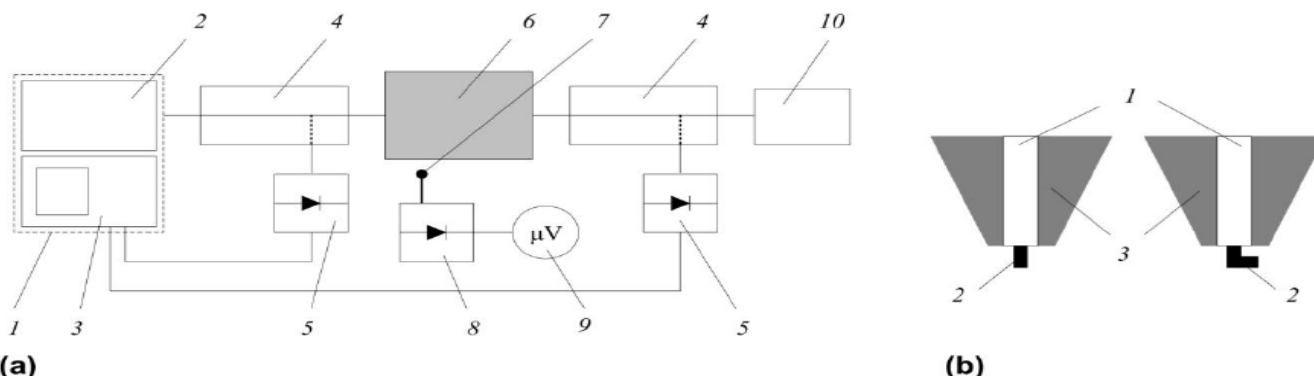


**Fig. 2. The Experimental Setup (a) and the Electric Probes (b).**

(a) 1 – scalar network analyzer; 2 – generator; 3 – indicator; 4 – directional couplers; 5 – build-in detectors; 6 – the structure under investigation; 7 – electric probe; 8 – waveguide detector; 9 – microvoltmeter; 10 – matched load; (b) 1 – semi-rigid coaxial cable; 2 – inner conductor; 3 – absorbing coating.

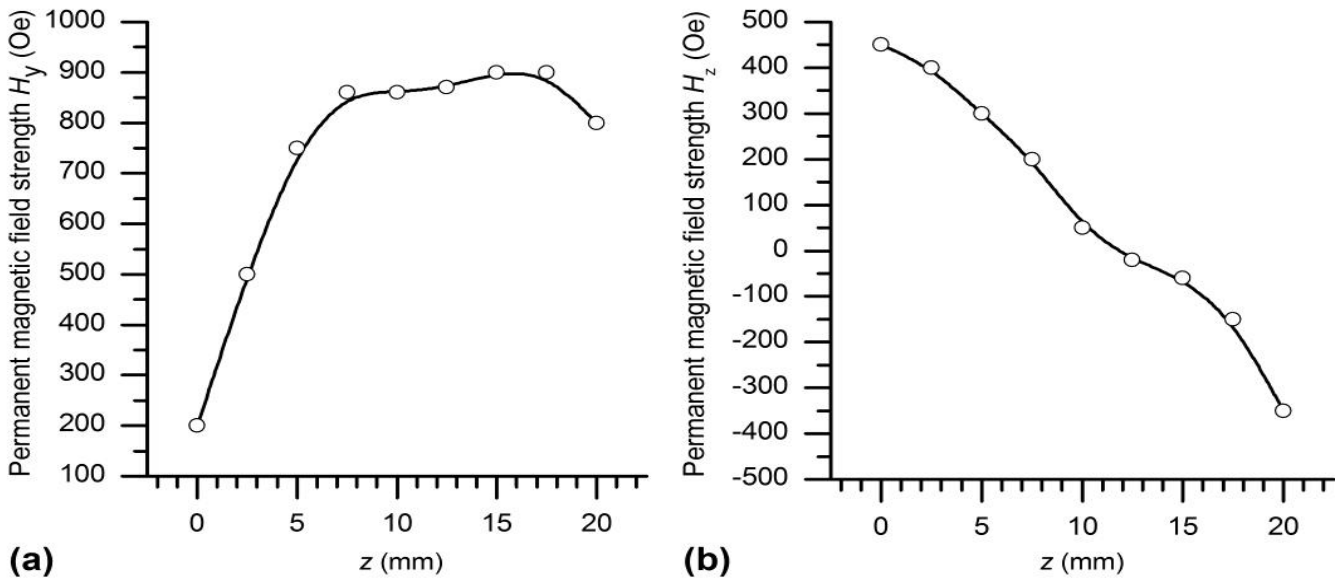


Fig. 3. The Transverse (a) and Longitudinal (b) Components of the Permanent Magnetic Field Strength.

The length of the probes is only few times lesser than the guide wavelength and that is the reason the positioning of the probe at a given coordinate always implies the averaging of the electric field component along the respective axis. In particular, the electric probe for the  $E_y$  component averages the electric field along the height above the IGs. The electric probes for the  $E_x$  and  $E_z$  components perform the averaging along the  $Ox$  and  $Oz$  axes, respectively. Due to  $90^\circ$  bending, the electric probe for the  $E_x$  and  $E_z$  components is less precise in comparison to the electric probe for the  $E_y$  component and it register in some extent the  $E_y$  component as well. As we have noted earlier [7], the electric probe for the  $E_x$  and  $E_z$  component works appropriately when these components are comparable or greater in comparison to the  $E_y$  component.

#### IV. RESULTS AND DISCUSSION

The disk-shaped permanent magnet with a diameter of 20 mm has been positioned under the ground plane just down the ferrite bar. We have adjusted the position of the permanent magnet to achieve a proper nonreciprocal behavior of the CFDIG structure. Insertion losses equal to  $-2.5$  dB and an isolation equal to  $-16$  dB have been registered at a frequency of 34 GHz. The isolation better than  $-10$  dB has been measured in the frequency range (33.6–34.5) GHz. The corresponding insertion losses were about  $-3$  dB. The strength of the permanent magnetic field along the coupling length has been measured with a magnetometer. The distributions of the transverse component  $H_y$  and the longitudinal component  $H_z$  are shown in Fig. 3a and Fig. 3b, respectively. The transverse component  $H_y$  (Fig. 3a) is almost constant in the range of  $z = (7-18)$  mm. The longitudinal component  $H_z$  (Fig. 3b) is equal to zero in the middle of the coupled region and changes its sign (direction). The transverse component  $H_y$  is significantly greater than the longitudinal component everywhere except in the beginning of the coupled region at  $z = (0-4)$  mm. The measured distributions of the electric field components for forward direction of propagation are shown in Fig. 4. The values set in arbitrary units anywhere in Fig. 4 (and in Fig. 5)

are proportional to the square of the respective components of the electric field, which results from the used square-law detector  $\delta$  (Fig. 2). The measurements have been completed at a frequency of 34 GHz, when relatively low losses equal to  $-2.5$  dB have been registered. The  $E_y$  component (Fig. 4a, b) has maxima at the beginning and at the end of the primary IG. These maxima correspond to the fact that the  $E_y$  component is the main electric field component of the dominant mode  $E_{y11}$  on the primary IG, which has been excited with the help of the SMRW-IG transitions used (Fig. 1). The  $E_y$  component has another local maxima in the middle of the secondary IG as well, that reveals coupling between dielectric and ferrite IGs with period of power transfer  $L$  equals to a half coupling length  $l/2$ . The energy comes gradually from primary dielectric IG to the secondary ferrite IG (from  $z = 0$  to  $z = l/2$ ) and returns back to the primary IG at  $z = l$ . The numerical investigation of the dominant mode on magnetized ferrite IG [8] has shown that at transverse magnetization perpendicular to the ground plane there is a growth of the  $E_x$  component in comparison to the pure  $E_{y11}$  mode on the dielectric IG. The measured distribution of the  $E_x$  component in the coupled region shown in Fig. 4c, d has confirmed this. As can be seen from Fig. 4c, d, the  $E_x$  component is the largest electric field component in the secondary ferrite IG. It has two big maxima near to the middle of the coupling length (at  $z = 8.5$  mm and  $z = 11.5$  mm), which is relevant to the coupling with period of power transfer  $L = l/2$ . Together with the  $E_y$  component, the  $E_z$  component is one of the two main electric field components of the dominant mode  $E_{y11}$  on the dielectric IG [6]. That is the reason the  $E_z$  component has the largest values at both ends of the primary IG (Fig. 4e, f). In the secondary IG the  $E_z$  component has local maximum at about  $z = 6$  mm (Fig. 4e, f). This is in accordance with the fact that the  $E_z$  component is the largest electric field component in longitudinally magnetized ferrite IG [8], and in the beginning of the secondary ferrite IG the longitudinal component of the permanent magnetic has significant value (Fig. 3). Another maximum of the  $E_z$  component in the secondary IG exists at its end (Fig. 4e, f). It is due to the fact that the end of the

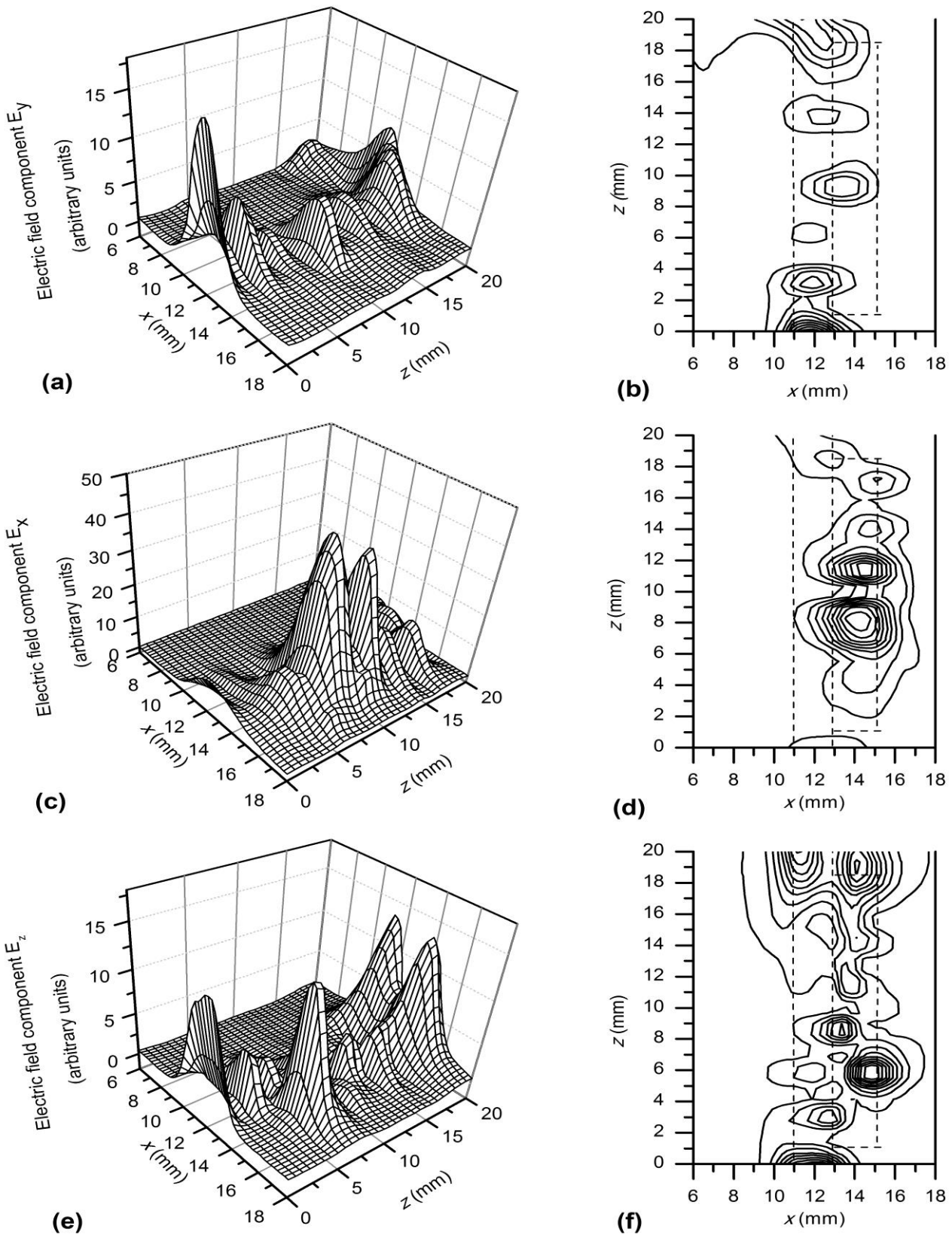


Fig. 4. The distribution of the electric field components along the coupling length in forward direction of propagation. (a, b)  $E_y$  component; (c, d)  $E_x$  component; (e, f)  $E_z$  component. Dashed line represents the outlines of the CFDIG structure.

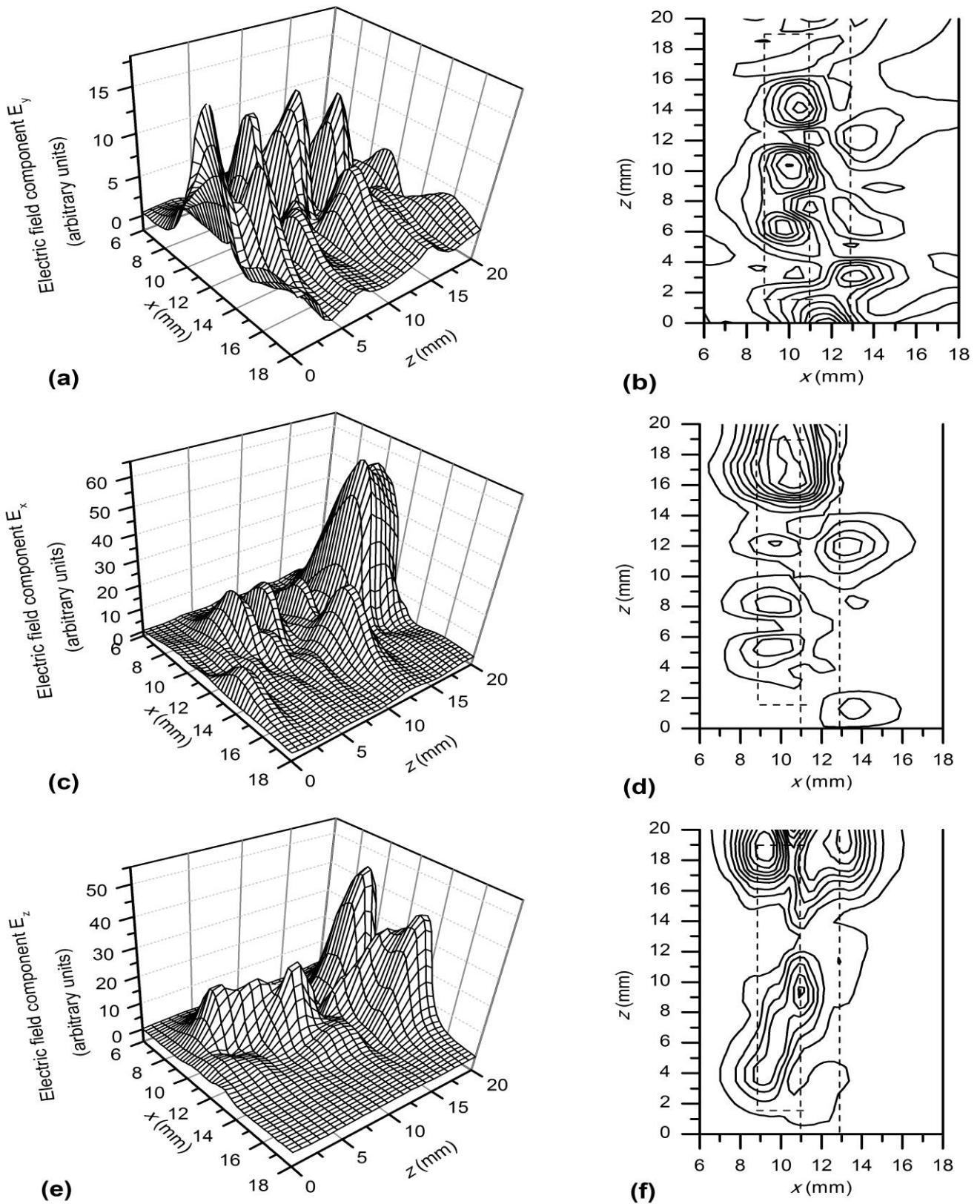


Fig. 5. The distribution of the electric field components along the coupling length in backward direction of propagation.

(a, b)  $E_y$  component; (c, d)  $E_x$  component; (e, f)  $E_z$  component. Dashed line represents the outlines of the CFDIG structure.

Secondary IG represents strong irregularity, which produces some radiation. The earlier investigation [9] has revealed that radiation effects in open ended IG structures are associated mainly with the  $E_z$  component.

The measured distributions of the electric field components for backward direction of propagation are shown in Fig. 5. The measurements have been completed also at a frequency of 34 GHz, when an isolation equal to  $-16$  dB have been registered. The  $E_y$  component (Fig. 5a, b) has relatively low values in the whole primary IG except its beginning ( $z = 0$ ). There are well expressed equidistant maxima in the secondary IG at  $z = 6$  mm,  $z = 10$  mm and  $z = 14$  mm. In this part of the coupling length ( $z = 6-14$  mm) the transverse component of the permanent magnetic field predominates over the longitudinal one (Fig. 3). The maxima observed in the secondary IG express the fact of effective coupling between primary and secondary IGs. They represent standing wave pattern, which is result of reflection from the ends of the secondary IG.

The absolute maximum of the  $E_x$  component in backward direction takes place at the end of the coupling length ( $z = 14-20$  mm) and covers both primary and secondary IGs (Fig. 5c, d). This maximum shows coupling between dielectric and ferrite IGs with period of power transfer  $L$  equal to a coupling length  $l$ . There are well defined weaker maxima of the  $E_x$  component in the secondary ferrite IG at about  $z = 5$  mm,  $z = 8$  mm and  $z = 12$  mm. The last maximum at  $z = 12$  mm covers the primary IG as well. This picture results from the reflections taking place at the end of the coupled region because of the fact that the wave with  $E_x$  component cannot propagate on the single mode primary dielectric IG and cannot pass through the SMRW-IG transitions as well. This situation can be described by consideration of the coupled region as an effective resonator for the  $E_x$  component.

The distribution of the  $E_z$  component in backward direction of propagation is shown in Fig. 5e, f. It is evident that the  $E_z$  component has its greatest values at the end of the coupled region, at  $z = 14-20$  mm. There are two reasons responsible for this distribution. Firstly, in backward direction these coordinates correspond to the part of the coupled region with considerable longitudinal magnetization and, as has been stated earlier, the largest electric field component of the dominant mode on longitudinally magnetized ferrite IG is namely the  $E_z$  component. Secondly, at the end of the secondary IG radiation effects exist with  $E_z$  being the main component of the radiated wave.

### V. CONCLUSION

The experimental investigation of coupled ferrite-dielectric image guide structure with in homogeneously magnetized ferrite element has been completed with the help of electric probes. At a frequency of 34 GHz the structure possesses a nonreciprocal behavior with insertion losses and isolation equal to  $-2.5$  dB and  $-16$  dB, respectively. The distributions of all three electric field components in forward and backward direction of propagation have been measured. These distributions reveal a nonreciprocal coupling between dielectric and ferrite image guides. In forward direction of propagation the period of power transfer  $L$  equals to a half coupling length  $l/2$  while in backward direction it is two times greater and equals to the

coupling length  $l$ .

The measurement of the permanent magnetic field has shown that the transverse component, which is perpendicular to the ground plane predominates over the longitudinal one almost in the whole coupled region. The earlier numerical study has shown that the propagating wave on ferrite image guide at this magnetization has additional main electric field component  $E_x$ . The measured distributions in this investigation have confirmed this. Due to the single mode operation of the primary dielectric image guide with the mode  $E_{y11}$ , the coupled region represents an effective resonator for the  $E_x$  component. The measured distributions have also shown that radiation with main component  $E_z$  exists at the ends of the secondary image guide, and this is in accordance with our earlier investigation of radiation effects in open image guide structures. The future work will aim to properly model and to investigate numerically the coupled ferrite-dielectric image guide structure with inhomogeneous magnetization.

### REFERENCES

1. A. S. Akyol and L. E. Davis, "Measurements of a leaky-wave ferrite isolator", IEEE Transactions on Microwave Theory and Techniques, vol. 51, May 2003, pp. 1476-1481.
2. P. Kwan and C. Vittoria, "Scattering parameters measurement of a nonreciprocal coupling structure", IEEE Transactions on Microwave Theory and Techniques, vol. 41, April 1993, pp. 652-657.
3. S. V. Belyakov, S. S. Gigoyan, and B. A. Murmuzhev, "Wideband isolators for measurements in millimeter wave range" (in Russian). Elektonnaya tehnika, vol. 419, May 1989, pp. 42-43.
4. I. I. Arestova and S. A. Ivanov "Nonreciprocal effects in coupled ferrite-dielectric image guide structures", in Proceedings of the 12<sup>th</sup> International Conference on Microwave Ferrites (ICMF). Gyulechica (Bulgaria), Sept. 1994, pp. 188-192.
5. E. A. J. Marcetili, "Dielectric rectangular waveguide and directional coupler for integrated optics", The Bell System Technical Journal, Sept. 1969, pp. 2071-2102.
6. I. Arestova, R. Tomova, and G. Angelova, "The dispersion and components of the dominant mode on the image guide for millimeter waves", Annuaire de l'Universite de Sofia "St. Kliment Ohridski", Faculte de Physique, vol. 103, 2010, pp. 5-17.
7. I. I. Arestova, P. I. Dankov, and V. P. Levcheva, "A Study on the Coupled Image Guide Structures", in Proceedings of the Progress in Electromagnetics Research Symposium (PIERS). Moscow (Russia), August 2009, pp. 1204-1208.
8. I. Arestova, "Computer aided investigation of the dominant mode on the homogeneously magnetized ferrite image guide", Annuaire de l'Universite de Sofia "St. Kliment Ohridski", Faculte de Physique, vol. 111, 2018, pp. 41-50.
9. I. I. Arestova, V. P. Levcheva, and P. I. Dankov, "Radiation Effects in Image Guide Structures", in Proceedings of the Telecommunication Forum (TELFOR). Belgrade (Serbia), Nov. 2009, pp. 903-906.

### AUTHOR PROFILE



**Iliyana Arestova** was born in Pernik, Bulgaria. She received her M.Sc. in Radiophysics and Electronics from St. Kliment Ohridski University of Sofia, Sofia, Bulgaria (1987). She has been at the Department of Radiophysics and Electronics, Faculty of Physics, St. Kliment Ohridski University of Sofia, Sofia, Bulgaria since 1996. Until the year 2016 she worked as assistant professor. She is author of tutorials for practical work on Basic Electronics, Oscillations and Waves, Radiation and Propagation of Electromagnetic Waves. She has been working on her Ph.D. Her research interests include ferrite devices for millimeter waves and antennas.





**Rositsa Tomova** was born in Kazanlak, Bulgaria. She received her M.Sc. in Measuring Electronics from St. Kliment Ohridski University of Sofia, Sofia, Bulgaria (1999). She works at Atanas Damyanov Vocational High School, Nikolaevo, Bulgaria. Her research interests include measurements in electronics.